

Supporting Information

Broadband near-infrared Cr³⁺-doped phosphor applied to near-infrared Light-Emitting Diodes: enhance luminescence and thermal stability by an annealing design

Tao Tan,^{a,b} Ran Pang,^{a,*} Shangwei Wang,^a Haiyan Wu,^a Jiutian Wang,^{a,b} Su Zhang,^{a,b} Chengyu Li,^{a,b,*} and Hongjie Zhang^a

a State Key Laboratory of Rare Earth Resource Utilization, Changchun Institute of Applied Chemistry, Chinese Academy of Sciences, Changchun 130022, P. R. China.

b University of Science and Technology of China, Hefei 230026, P. R. China

* Corresponding authors.

E-mail addresses:

pangran@ciac.ac.cn (Ran Pang)

Number of pages: 18

Number of figures: 17

Number of tables: 3

Table S1 Rietveld Parameters

	LMS host	LMS:0.03Cr ³⁺
a = b = c	4.2463 Å	4.2457 Å
A = β = γ	90°	90°
Volume	76.57 Å ³	76.53 Å ³
R _{wp}	10.48 %	7.84 %
R _p	7.63 %	5.73 %
χ ²	1.711	2.04
Crystal	Cubic	Cubic
Space group	<i>Fm</i> $\bar{3}$ <i>m</i>	<i>Fm</i> $\bar{3}$ <i>m</i>

Table S2 Rietveld Parameters

	LMS:0.03Cr ³⁺	After annealing
a = b = c	4.2457 Å	4.2470 Å
A = β = γ	90°	90°
Volume	76.53 Å ³	76.60 Å ³
R _{wp}	7.84 %	6.79 %
R _p	5.73 %	5.34 %
χ ²	2.04	1.95
Crystal	Cubic	Cubic
Space group	<i>Fm</i> $\bar{3}$ <i>m</i>	<i>Fm</i> $\bar{3}$ <i>m</i>

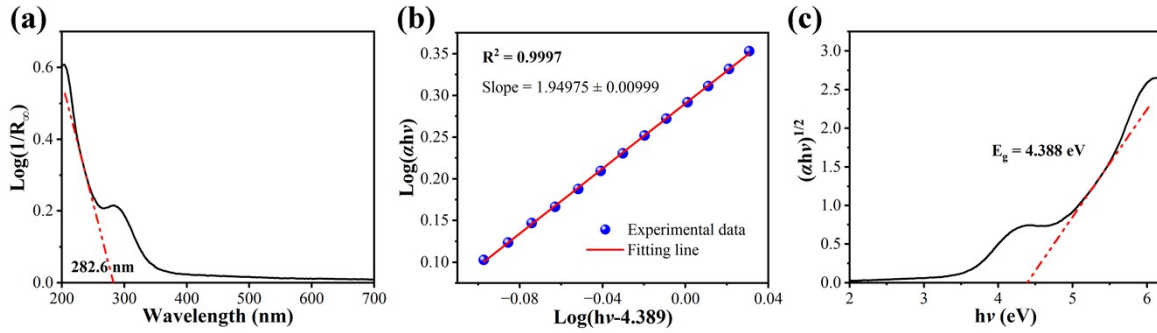


Fig. S1. Determination of the band gap of $\text{Li}_2\text{Mg}_3\text{SnO}_6$.

The band gap of $\text{Li}_2\text{Mg}_3\text{SnO}_6$ can be estimated according to Equation S1.[1, 2]

$$\alpha hv = A(hv - E_g)^{n/2} \quad (\text{S1})$$

Where hv is the photon energy; E_g is the value of the band gap; $n = 1$ for a direct band-gap; $n = 4$ for an indirect band-gap. This Equation can be derived as:

$$\text{Log}(\alpha hv) = (n/2)\text{Log}(hv - E_g) + \text{Log}(A) \quad (\text{S2})$$

The spectrum similar to the absorption spectrum is converted from the DR spectrum (Fig. S1a).

An approximate E_g is estimated as 4.389 eV. According to the derived formula, the slope of $\text{Log}(\alpha hv)$ vs. $\text{Log}(hv - E_g)$ is fitted with a liner equation to give the value of n . As shown in Fig. S1b, n value is calculated to be 4. Thus, $\text{Li}_2\text{Mg}_3\text{SnO}_6$ has an indirect band gap. From the linear extrapolation of the function $(\alpha hv)^{1/2} = 0$, as shown in Fig. S1c, the indirect optical band gap is estimated to be 4.388 eV.

Estimation of Huang–Rhys factor S and phonon energy $\hbar\omega$.

The estimation of Huang–Rhys factor S and phonon energy $\hbar\omega$ has been completed by the method proposed by Zundu Luo.[3] For the point of Zundu Luo, the electron-phonon coupling is in fact a multi-mode interaction, and the usual single-mode model is too simple to describe physical reality. Meanwhile, at that time, most of the spectral data were obtained at room temperature or 77 K, but almost all the estimations of S and $\hbar\omega$ published are based on a formula for 0 K. A model can take into account these two facts was proposed. According to the PLE and PL spectra, the FWHM and Stokes shift ΔS have been obtained. And ratio of $(FWHM)^2$ and $(\Delta S/2)$ is calculated.

$$r = \frac{(FWHM)^2}{\frac{\Delta S}{2}} = 2 \frac{(FWHM)^2}{\Delta S} \quad (S3)$$

And, the Stokes shift ΔS is

$$\Delta S = E(^4A_2 \rightarrow ^4T_2) - E(^4T_2 \rightarrow ^4A_2) = 2S\overline{\hbar\omega} \quad (S4)$$

The average phonon energy $\hbar\omega$ can be defined as

$$\overline{\hbar\omega} = \frac{1}{S} \sum_k \left(\frac{\omega_k}{2\hbar} \right) \Delta_{jik}^2 (\hbar\omega_k) \quad (S5)$$

$$S = \sum_k \left(\frac{\omega_k}{2\hbar} \right) \Delta_{jik}^2 \quad (S6)$$

For high temperature and under strong coupling condition,

$$FWHM = \left[8 \ln 2 \times S(T) \overline{(\hbar\omega)^2} \right]^{1/2} = 2.3548 \left[S(T) \overline{(\hbar\omega)^2} \right]^{1/2} \quad (S7)$$

where

$$S(T) = \sum_k \Delta_{jik}^2 \left(\frac{\omega_k}{2\hbar} \right) \coth \left(\frac{\beta \hbar \omega_k}{2} \right) \quad (S8)$$

and

$$\overline{(\hbar\omega_k)^2} = \frac{1}{S(T)} \sum_k \left[\Delta_{jik}^2 \left(\frac{\omega_k}{2\hbar} \right) \coth \left(\frac{\beta \hbar \omega_k}{2} \right) \right] (\hbar\omega_k)^2 \quad (S9)$$

Therefore, the formula of ratio between $(\text{FWHM})^2$ and $(\Delta S/2)$ is given below:

$$r = \frac{5.545 \sum_k \left[\Delta_{jik}^2 \left(\frac{\omega_k}{2\hbar} \right) \coth \left(\frac{\beta \hbar \omega_k}{2} \right) \right] (\hbar \omega_k)^2}{\sum_k \Delta_{jik}^2 \left(\frac{\omega_k}{2\hbar} \right) (\hbar \omega_k)} \quad (\text{S10})$$

A model consisting of five multi-frequency patterns is used here. Let their frequencies differ by a fixed multiple factor. And the product $S_k \hbar \omega_k$ (for $k = 1, 2, 3, 4, 5$) can be described as following equation, where $\hbar \omega_k = k \hbar \omega_1$ for $k = 1, 2, 3, 4, 5$.

$$S_k (\hbar \omega_k) = \Delta_{jik}^2 \left(\frac{\omega_k}{2\hbar} \right) (\hbar \omega_k) = \frac{1}{5} \sum_k \Delta_{jik}^2 \left(\frac{\omega_k}{2\hbar} \right) (\hbar \omega_k) \quad (\text{S11})$$

At room temperature $\beta = 1/kT = 0.005 \text{ cm}^{-1}$ (More precise values can also be taken here, $\beta = 1/kT = 0.0047965 \text{ cm}^{-1}$ at $T = 300 \text{ K}$). Therefore, the ratio of $(\text{FWHM})^2$ and $(\Delta S/2)$ is calculated by the simplified formula.

$$r = 1.109 \sum_{k=1}^5 \left[\coth (0.0025 k \hbar \omega_1) (k \hbar \omega_1) \right] \quad (\text{S12})$$

Using the values of ratio obtained by spectral measurements and Equations (S3 and S4), it is easy to determine $\hbar \omega_1$ by Equation (S10). Then S_1 , S and $\overline{\hbar \omega}$ can be obtained by following Equation.

$$S_1 \hbar \omega_1 = \frac{1}{5} (S \hbar \omega) = \frac{1}{10} \Delta S \quad (\text{S13})$$

$$S = S_1 \left(1 + \frac{1}{2} + \frac{1}{3} + \frac{1}{4} + \frac{1}{5} \right) = 2.28 S_1 \quad (\text{S14})$$

$$\overline{\hbar \omega} = \frac{\Delta S}{2S} \quad (\text{S15})$$

For our phosphor LMS:0.03Cr^{3+} , the ${}^2\text{E} \rightarrow {}^4\text{A}_2$ (R line) and ${}^4\text{T}_2 \rightarrow {}^4\text{A}_2$ (broadband) transitions coexist in the emission spectrum. Therefore, only approximate evaluations can be made here.

This method is based on the premise of strong electron-phonon coupling approximation, which may not be suitable for phosphors with both R line and broadband transitions. The calculations here are just to provide a reference. Through the method of deconvolution, an approximate

value of $E(^4T_2 \rightarrow ^4A_2)$ is obtained, which is about 12502.4 cm^{-1} . And FWHM is about 2886.6 cm^{-1} . According to excitation spectrum, the value of $E(^4A_2 \rightarrow ^4T_2)$ is about 16260.2 cm^{-1} . Therefore, at the condition of $T = 300\text{K}$ ($\beta = 1/kT = 0.0047965 \text{ cm}^{-1}$), $\hbar\omega_1$ and S_1 are calculated to be 239.69 cm^{-1} and 1.5678 . So, the Huang–Rhys factor S and average phonon energy $\overline{\hbar\omega}$ of LMS:0.03Cr^{3+} phosphor are evaluated to be 3.57 and 525.63 cm^{-1} .

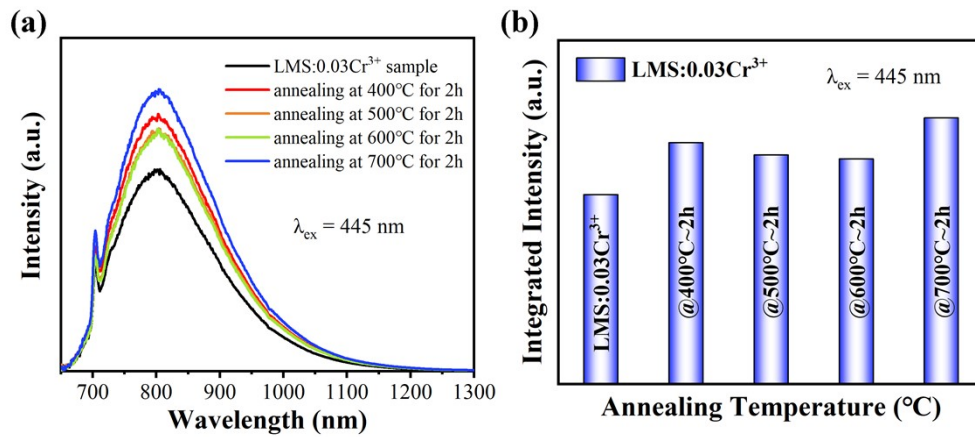


Fig. S2. (a) PL spectra of LMS:0.03Cr^{3+} sample with different annealing temperatures. (b) Integrated intensity of LMS:0.03Cr^{3+} sample with different annealing temperatures.

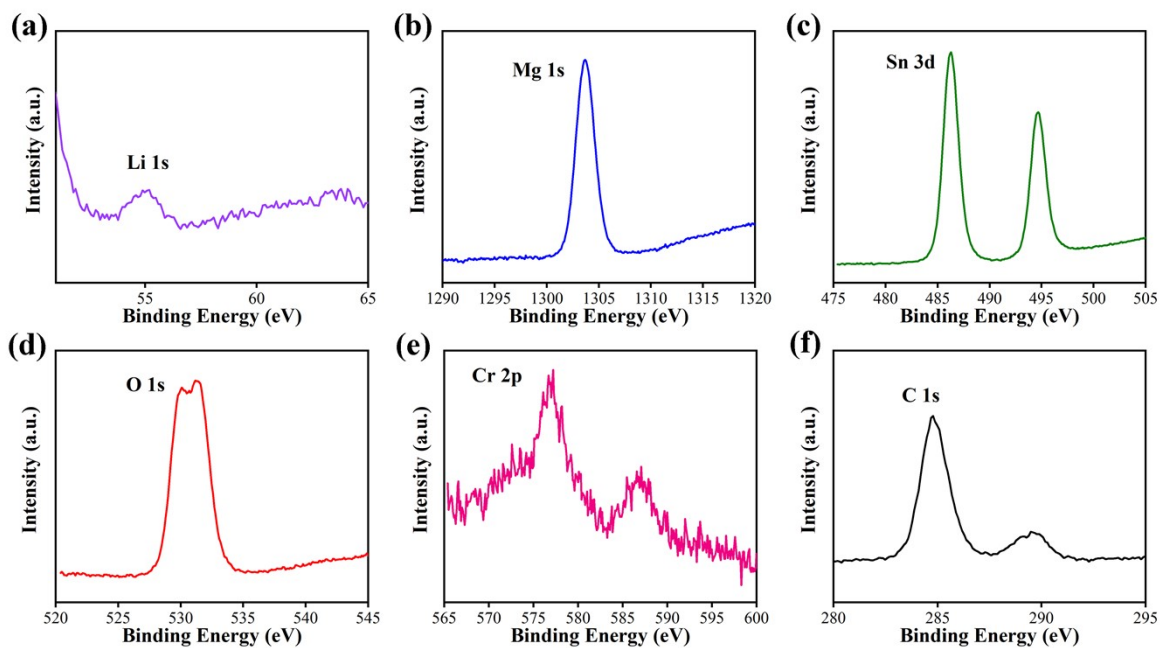


Fig. S3. X-ray Photoelectron Spectroscopy (XPS) of LMS:0.03Cr³⁺ sample.

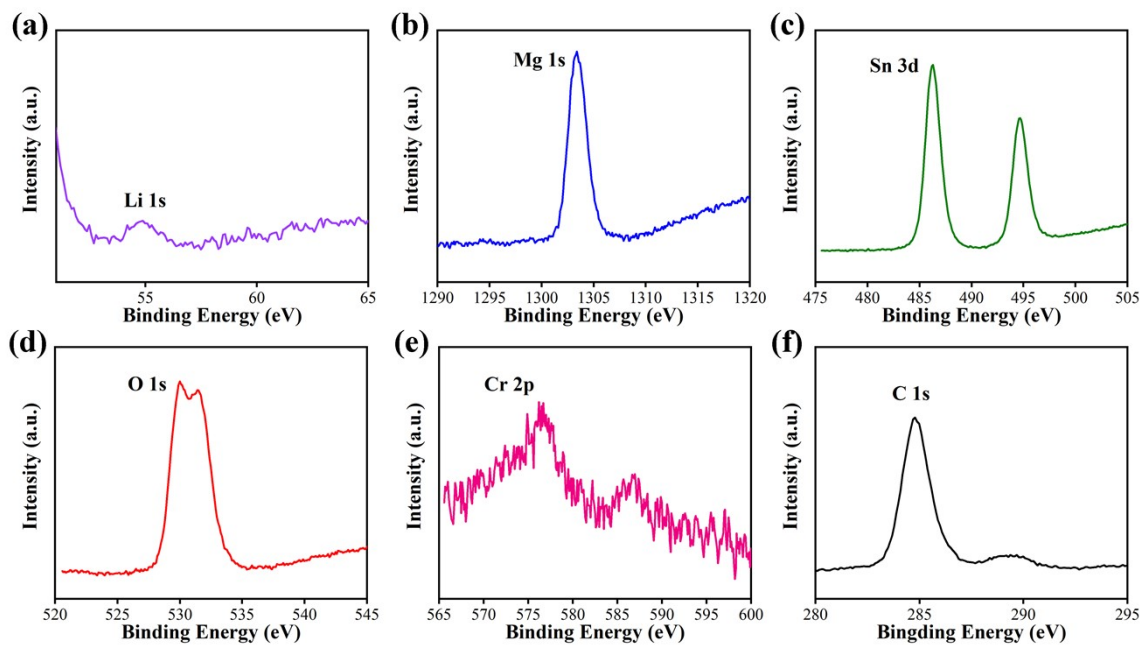


Fig. S4. X-ray Photoelectron Spectroscopy (XPS) of optimized aLMS:0.03Cr³⁺ sample.

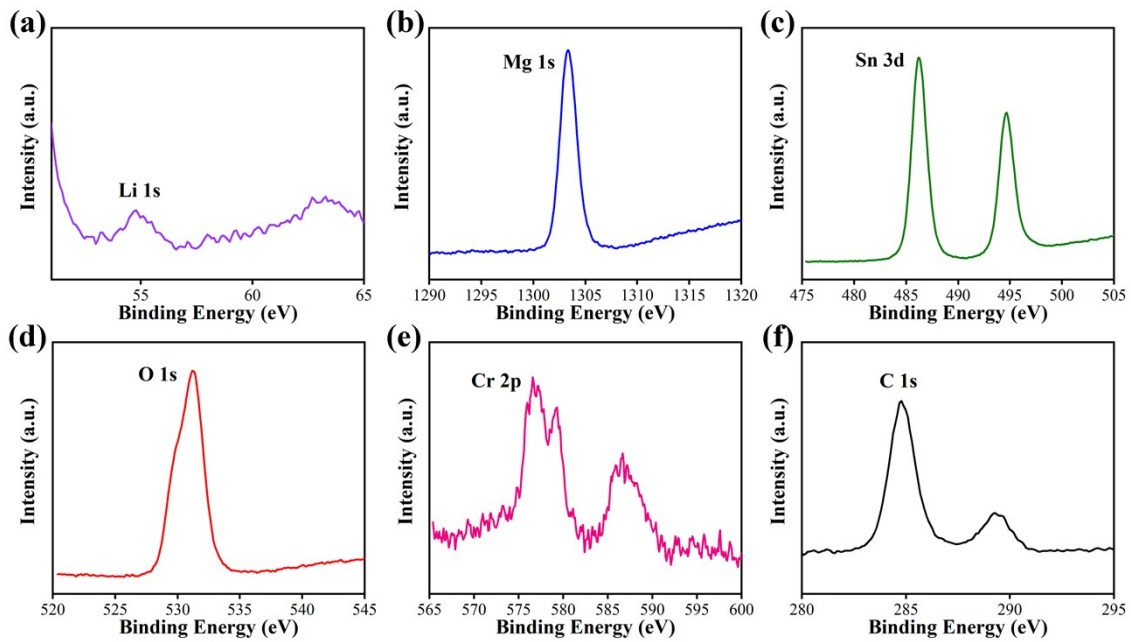


Fig. S5. X-ray Photoelectron Spectroscopy (XPS) of LMS:0.1Cr³⁺ sample.

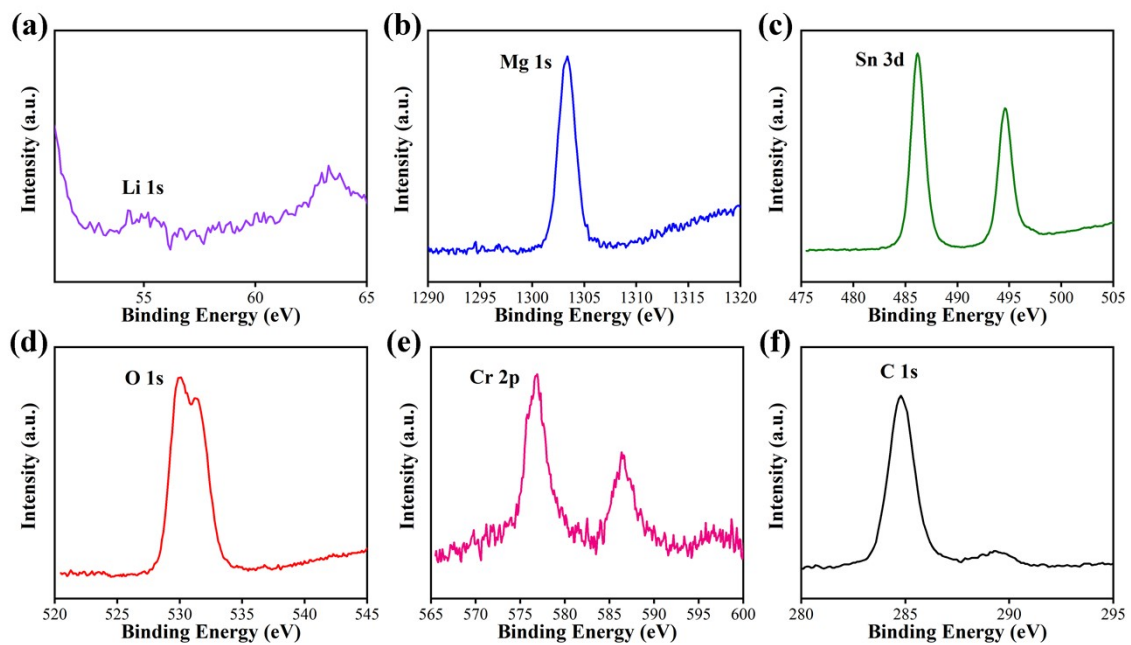


Fig. S6. X-ray Photoelectron Spectroscopy (XPS) of optimized aLMS:0.1Cr³⁺ sample.

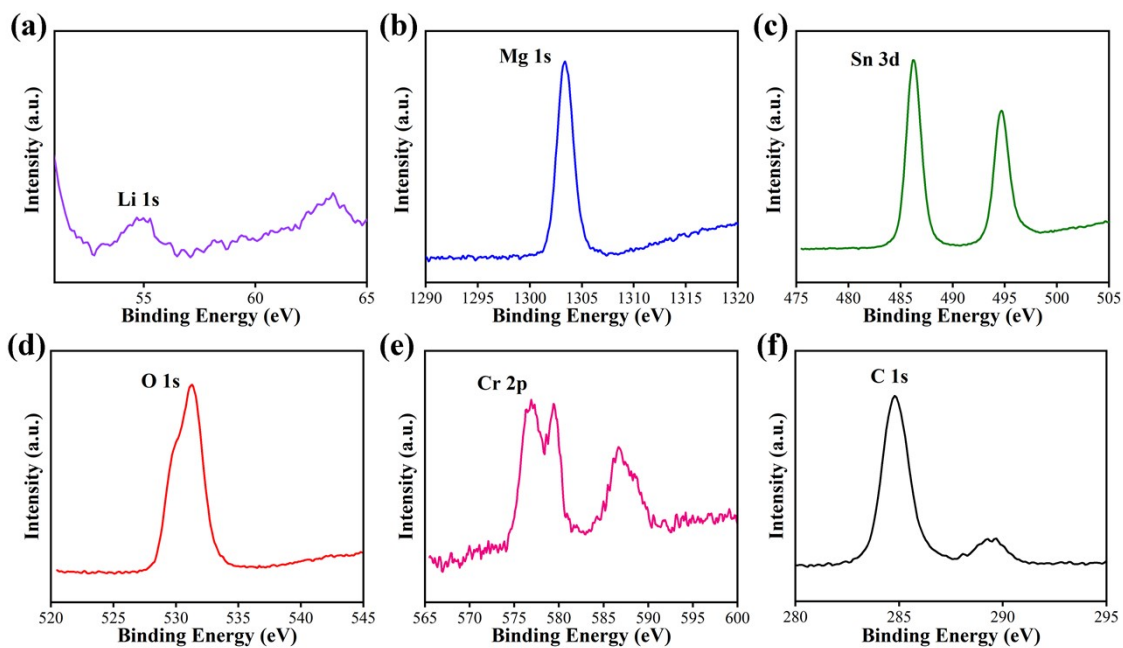


Fig. S7. X-ray Photoelectron Spectroscopy (XPS) of LMS:0.2Cr³⁺ sample.

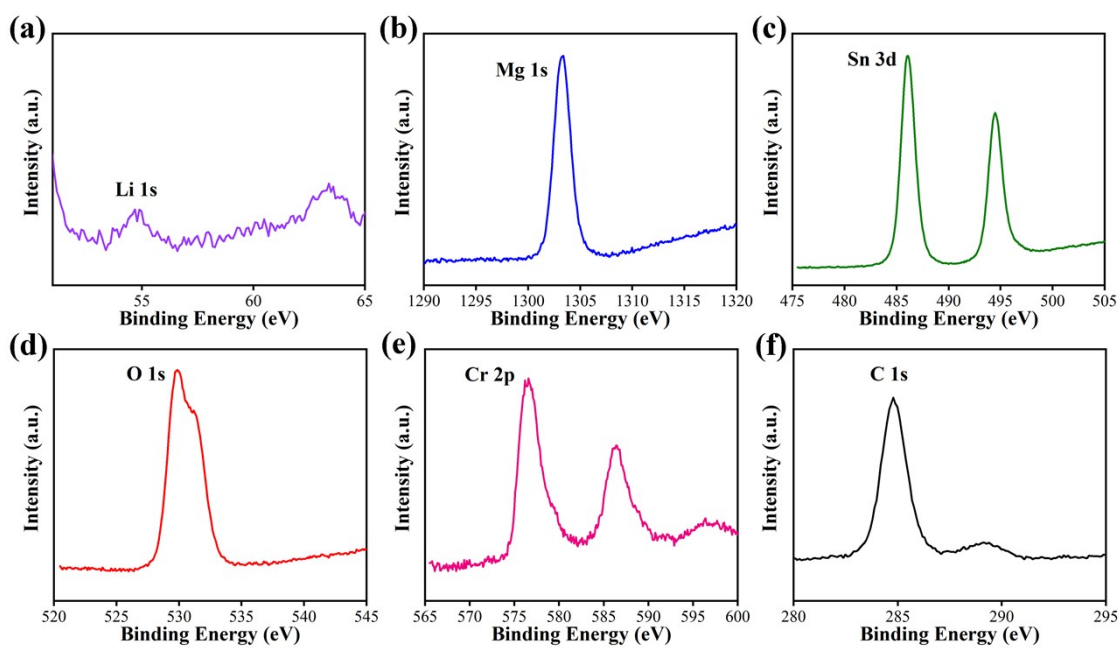


Fig. S8. X-ray Photoelectron Spectroscopy (XPS) of optimized aLMS:0.2Cr³⁺ sample.

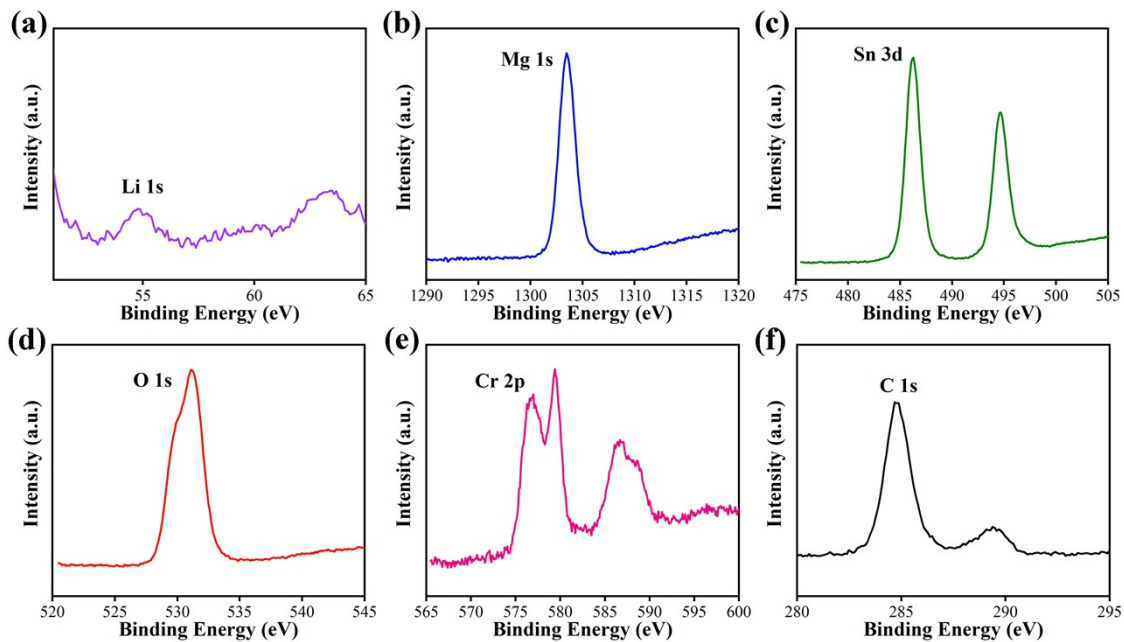


Fig. S9. X-ray Photoelectron Spectroscopy (XPS) of LMS:0.3Cr³⁺ sample.

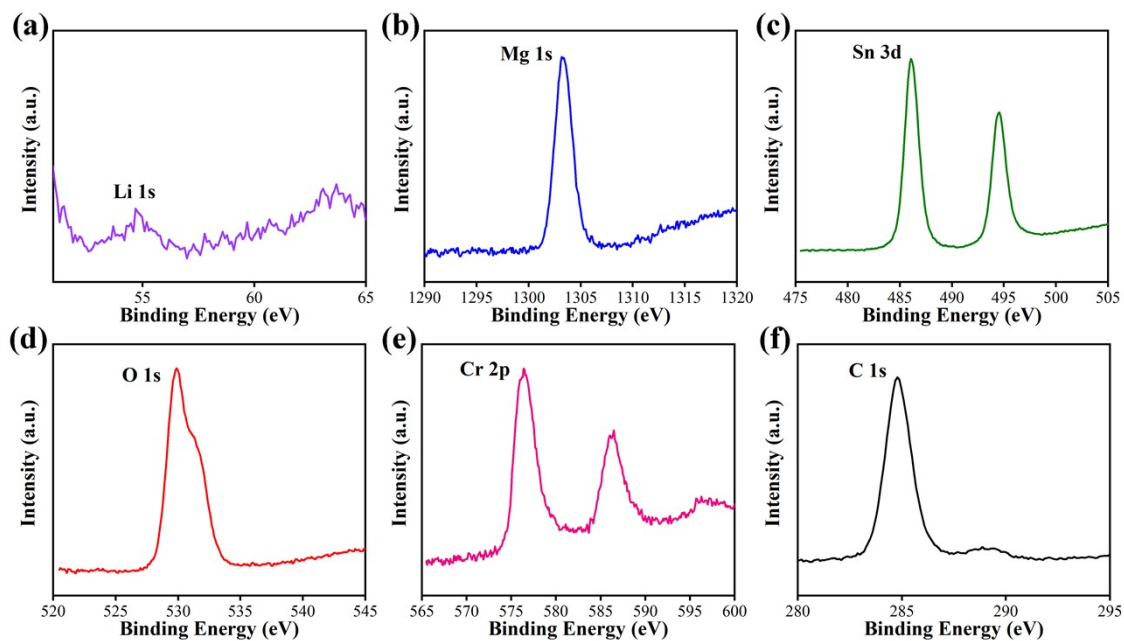


Fig. S10. X-ray Photoelectron Spectroscopy (XPS) of optimized aLMS:0.3Cr³⁺ sample.

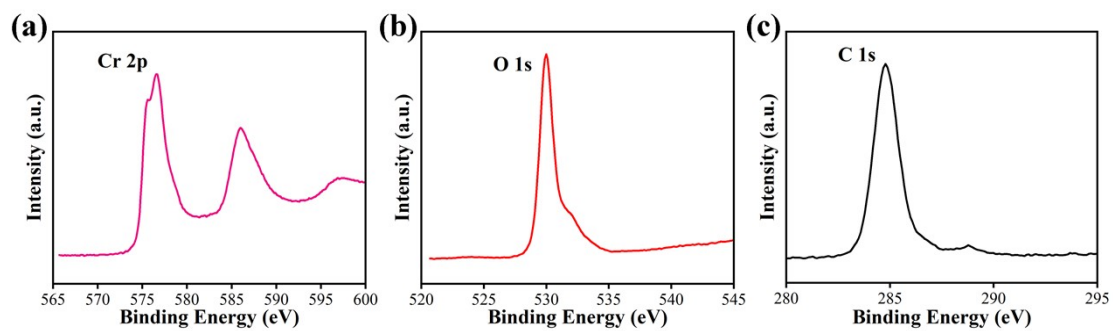


Fig. S11. X-ray Photoelectron Spectroscopy (XPS) of Cr_2O_3 sample.

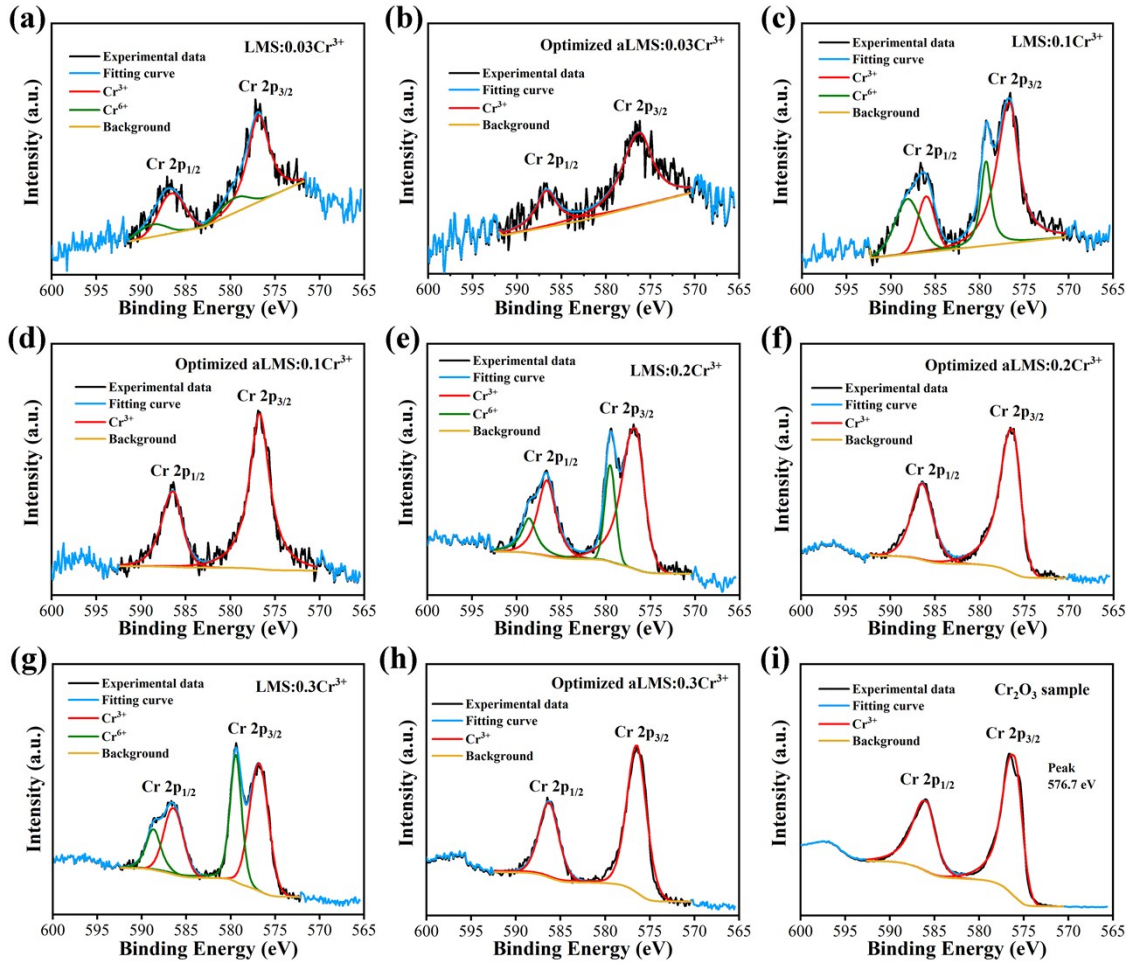


Fig. S12. Peak Fitting of Cr element in XPS.

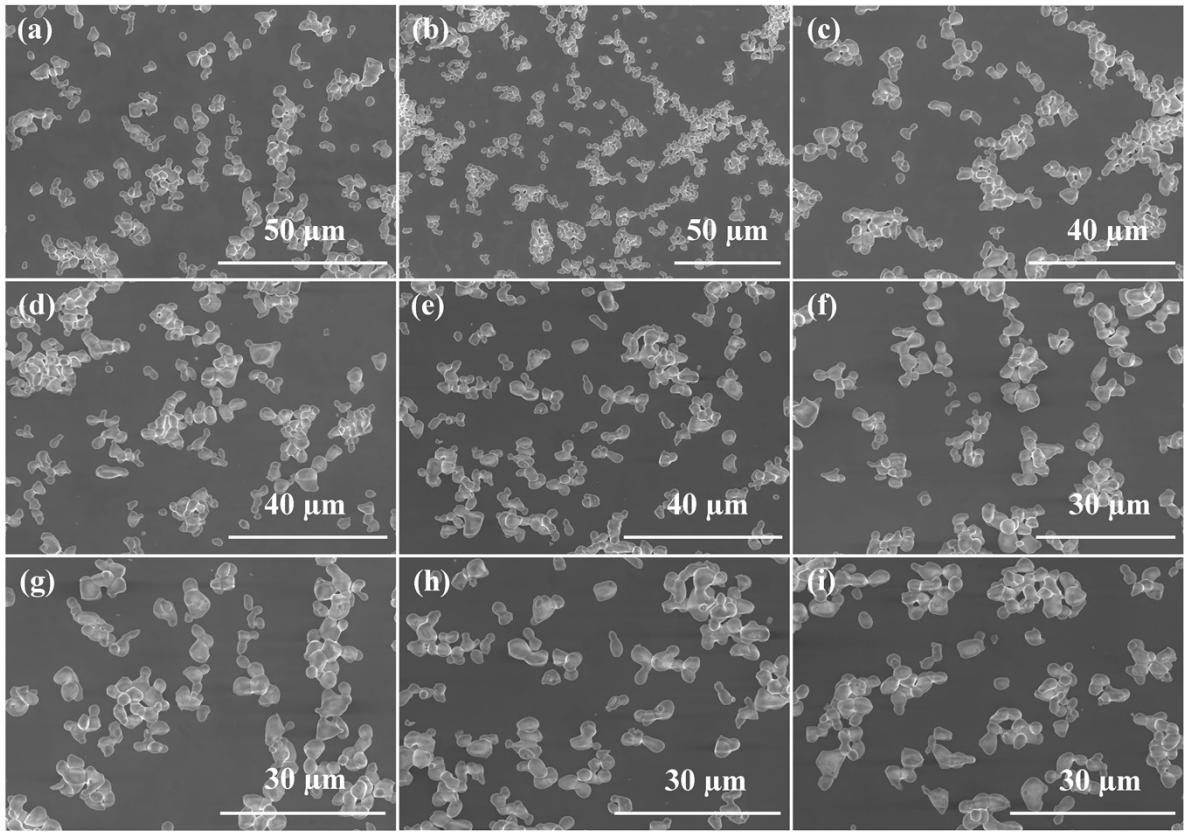


Fig. S13. SEM graphs of optimized aLMS:0.03Cr³⁺ sample.

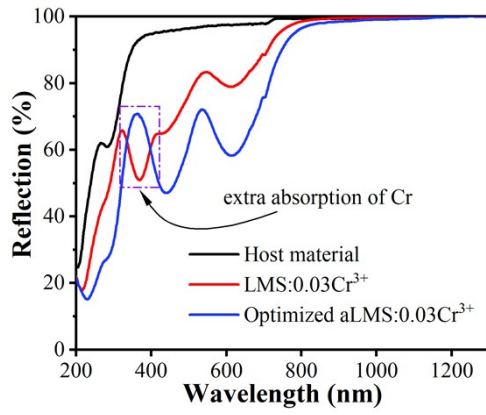


Fig. S14. The diffuse reflectance spectra of host material, LMS:0.03Cr³⁺ and Optimized aLMS:0.03Cr³⁺ samples.

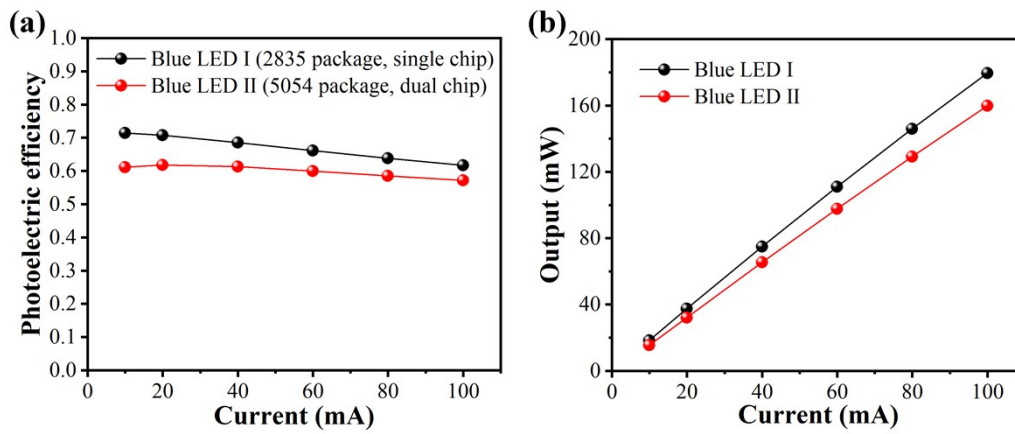


Fig. S15. (a) The photoelectric efficiency of Blue LED I and II at driving current of 10–100 mA. (b) The output power of Blue LED I and II at driving current of 10–100 mA.

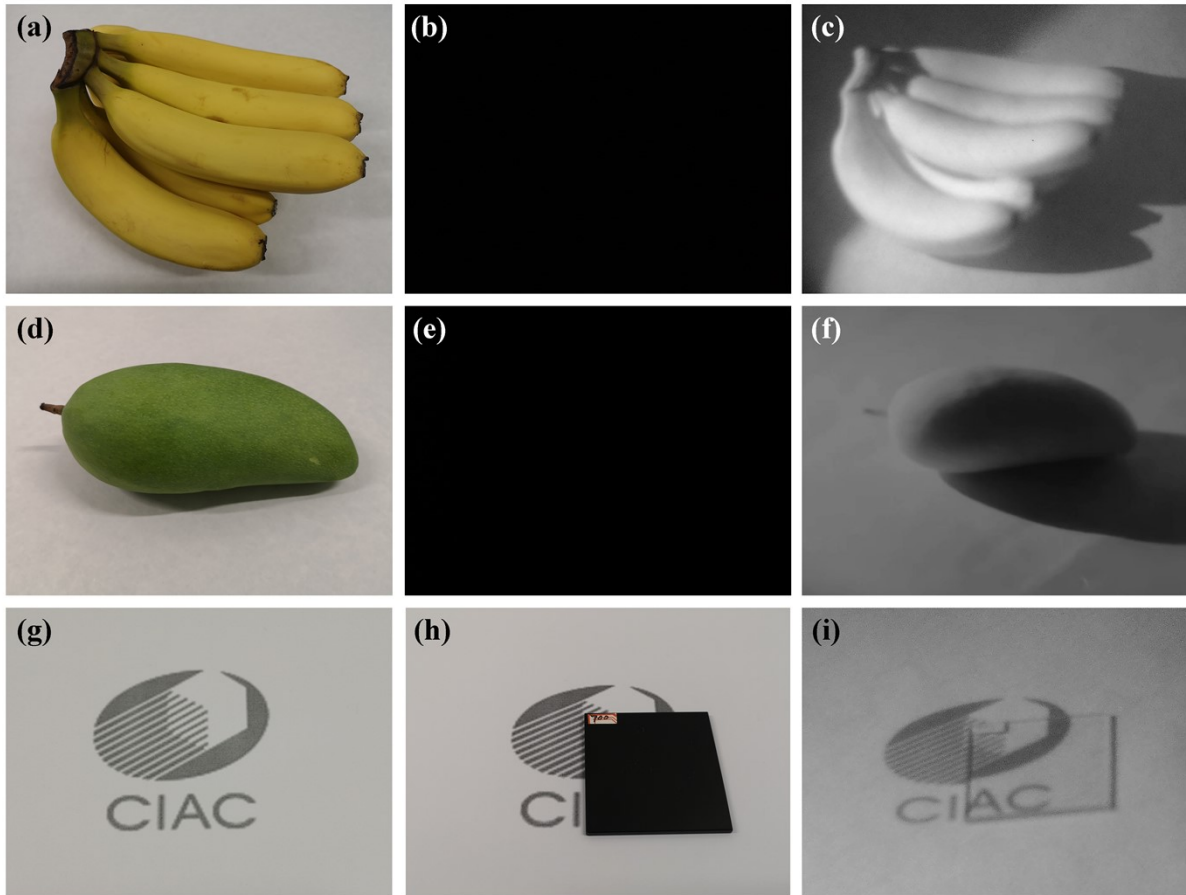


Fig. S16. The photographs of banana taken with camera (a) under indoor lighting and (b) in a dark environment. (c) A photograph of banana taken with NIR camera under NIR pc-LED lighting. The photographs of mango taken with camera (d) under indoor lighting and (e) in a dark environment. (f) A photograph of mango taken with NIR camera under NIR pc-LED lighting. The photographs of CIAC logo (g) unblocked by 700 nm filter and (h) blocked by 700 nm filter taken with camera under indoor lighting. (i) A photograph of CIAC logo taken with NIR camera under NIR pc-LED lighting.

The feasibility of NIR pc-LED prototype light source made of aLMS:0.03Cr³⁺ sample has been preliminarily verified through night vision and NIR imaging application.

Annealing design applied to Cr³⁺-doped phosphors

Table S3 Annealing treatment in reducing atmosphere

Samples	Improvement of integrated intensity (emission spectra)
Ga _{3.98} GeO ₈ :0.02Cr ³⁺	9.1%
Ga _{3.9} GeO ₈ :0.1Cr ³⁺	8.0%
LiIn _{0.92} Ge ₂ O ₆ :0.08Cr ³⁺	4.6%
Mg ₂ SnO ₄ :0.02Cr ³⁺	17.9%
Mg _{1.4} Zn _{0.6} SnO ₄ :0.03Cr ³⁺	4.1%
K ₂ Ga _{1.97} Sn ₆ O ₁₆ :0.03Cr ³⁺	54.8%
Ga _{0.994} TaO ₄ :0.006Cr ³⁺	10.0%
Ga _{1.57} In _{0.4} O ₃ :0.03Cr ³⁺	24.1%
Li ₂ Mg ₃ TiO ₆ :0.03Cr ³⁺	23.3%
Li ₂ Mg ₃ SnO ₆ :0.03Cr ³⁺	47.0%
Li ₂ Mg ₃ SnO ₆ :0.06Cr ³⁺	58.0%
Li ₂ Mg ₃ SnO ₆ :0.1Cr ³⁺	32.4%
Li ₂ Mg ₃ SnO ₆ :0.3Cr ³⁺	66.0%

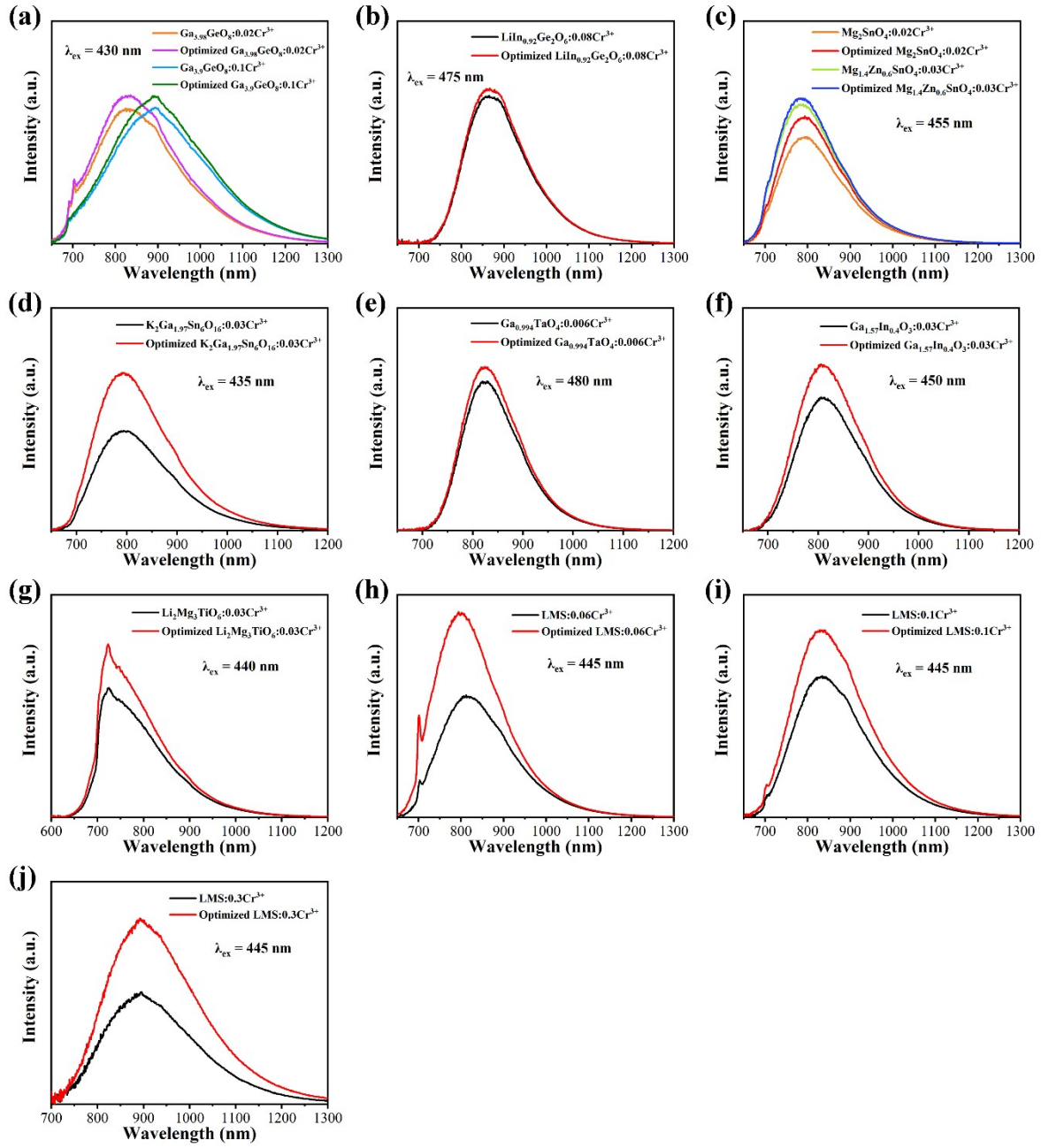


Fig. S17. PL spectra of different samples before and after annealing treatment.

References

- [1] L. L. Zhang, D. D. Wang, Z. D. Hao, X. Zhang, G. H. Pan, H. J. Wu, J. H. Zhang, *Adv. Opt. Mater.*, 2019, **7**, 1900185.
- [2] T. Tan, S. W. Wang, J. Y. Su, W. H. Yuan, H. Y. Wu, R. Pang, J. T. Wang, C. Y. Li, H. J. Zhang, *ACS Sustain. Chem. Eng.*, 2022, **10**, 3839-3850.
- [3] Z. D. Luo, Y. D. Huang, *J. Phys. Condens. Matt.*, 1992, **4**, 9751-9760.